

Spatial-Temporal Meta-path Guided Explainable Crime Prediction

Yuting Sun¹, Tong Chen¹ and Hongzhi Yin^{1*}

¹School of Information Technology and Electrical Engineering,
The University of Queensland, Australia.

*Corresponding author(s). E-mail(s): db.hongzhi@gmail.com;
Contributing authors: yuting.sun@uqconnect.edu.au;
tong.chen@uq.edu.au;

Abstract

Exposure to crime and violence can harm individuals' quality of life and the economic growth of communities. In light of the rapid development in machine learning, there is a rise in the need to explore automated solutions to crime prevention. The increasing availability of both fine-grained urban and public service data has driven a recent surge in fusing such cross-domain information to facilitate crime prediction. By capturing the information about social structure, environment, and crime trends, existing machine learning predictive models have explored the dynamic crime patterns from different views. However, these approaches mostly convert such multi-source knowledge into implicit and latent representations (e.g., learned embeddings of districts), making it still a challenge to investigate the impacts of explicit factors for the occurrences of crimes behind the scenes. In this paper, we present a **S**patial-**T**emporal **M**eta-path guided **E**xplainable **C**rime prediction (**STMEC**) framework to capture dynamic patterns of crime behaviours and explicitly characterize how the environmental and social factors mutually interact to produce the forecasts. Extensive experiments show the superiority of STMEC compared with other advanced spatial-temporal models, especially in predicting felonies (e.g., robberies and assaults with dangerous weapons).

Keywords: Crime Prediction, Spatial-temporal Modelling, Data Mining, Explainability

1 Introduction

Crime is an inevitable and persistent problem that brings negative outcomes to society. It is reported that worldwide homicide has caused more than 400,000 deaths each year. Given 80% of the victims are younger than 50 years old, homicide become one of the leading causes of death among young adults [1]. Apart from the long-lasting physical and psychological injuries the victims may suffer from, crime can also increase government expenditures on police protection and justice services. According to the report from the Australian Institute of Criminology, serious and organised crime has cost the Australian government up to 47.4 billion dollars in 2017 [2]. To minimize the effect on public safety and urban sustainability, rapid response policing is always required when government agencies are alerted on any criminal activities. In this case, crime prediction plays a key role in changing the situation from being blind-sided to being better prepared, and is formulated as the task of predicting region-wise crime rates using historical records.

As crime data is a type of spatial-temporal event data, some effective data mining techniques have been proposed to explore the spatial and temporal features of crimes. Temporal information in historical crime records concerning periodicity is emphasized by the routine activity theory [3]. Traditional time series models, such as Autoregression Integrated Moving Average (ARIMA) [4], Linear Regression and Support Vector Regression (SVR) [5] are widely used to make short-term crime forecasting. However, these models emphasize more on recent data and assume a fixed pattern of seasonality limited by linear models. Unlike typical time series such as traffic and weather, crime events have more irregularity in its temporal patterns, restricting the effectiveness of these conventional methods. Additionally, such methods fall short when capturing the spatial connections among regions, which are crucial as a region’s crime patterns can also be inferred via geographically adjacent [6] and structurally similar [7] regions. Though methods based on recurrent neural networks (RNNs) [8, 9] are proposed for crime prediction, they overlook the correlations between regions with either geographical [8] or semantic [9] (e.g., demographic structure) affinity. Thus, a model specifying the spatial-temporal dynamics of criminal behaviors is highly desired.

Based on the nature of crimes [10], both social characteristics and geographical locations of the residential places exhibit strong correlations with crimes. With the increasing availability of data collected from different channels, it has recently become possible to fuse multi-source information to facilitate crime prediction [11]. For example, [12] aggregates various resources by formulating them as graph-structured data and merging the learned graph representations. However, by merely treating the auxiliary information as the input feature for each region, it fails to fully account for the impact of each factor within the fine-grained urban data (e.g., income level and demographic distribution), leading to a substantial loss of context information. Meanwhile, it is non-trivial to fuse and represent the multi-faceted information in a more expressive way to quantify their varying contributions to different crime events.

The advances in latent factor models, especially neural networks, have witnessed dominating performance in predictive tasks where crime prediction is no exception. Those methods normally represent regions as implicit embedding through aggregating the information in both spatial and temporal domains [7–9, 13]. Despite the capability of forecasting the occurrence of crime events by capturing temporal patterns and neighborhood characteristics, the rationale behind the resulted predictions largely remain unexplainable within most methods [8, 9]. Understanding these factors that limit the communities from preventing crimes is of great importance to government agencies, as more effective measures can be taken to reduce crimes. While criminologists put a lot of effort into exploring reasons that cause crimes, the factors leading to criminal behaviors are still nowhere near well-understood [14]. Some methods with attention mechanisms [8] may distinguish the spatial and temporal effect on crime prediction, but the analysis on more specific factors (e.g., income level and population distribution) is left untouched, hindering both model performance and explanation quality. Apart from this, the importance of assumed factors may vary concerning different regions at different times. For example, even though economic and social disadvantages are believed to render areas crime-prone [14], rural areas with a lower level of urbanization are less likely to attract offenders [15]. However, most existing crime prediction methods do not differentiate such multifaceted information or further discuss the impact of features from multiple views [9, 12, 16, 17], while statistical learning methods (e.g., linear regression and decision trees) reap direct interpretability but sacrifice the prediction accuracy [18, 19].

To this end, we aim to predict the occurrence of crimes in each region by addressing the challenges in: (1) modeling the spatial-temporal effect; (2) expressively fusing multi-view information; and (3) providing interpretability on the causes of different crime types across regions. To address these challenges, we propose a novel framework - **S**patial-**T**emporal **M**eta-path guided **E**xplainable **C**rime prediction (**STMEC**). Different from existing graph based and grid based crime prediction models [7–9, 12, 13] that capture the relationships between regions through either geographical distance or venue based similarity, STMEC can: (1) encode temporal dynamics and semantic similarity among regions into their representations to improve performance; (2) project multifaceted dimensions of auxiliary data into a heterogeneous graph to capture rich context information; and (3) explicitly model the interactions between regions and features into a distribution-aware path to enhance explainability.

It is worth noting that STMEC novelly depicts the relations between regions by different social and environmental factors, and its expected performance and explainability are strengthened via the path-enriched features in the graph-structured data. The idea is inspired by the findings from prior works mentioned above, which suggest that similar urban features or adjacent locations of regions will lead to similar crime patterns [6, 7]. To complement the problem of fusing multifaceted information in our model, we characterize the interactions between regions and features by leveraging the concept of the

meta-path [20]. Compared with existing crime prediction methods [8, 9, 12] that merely treat multi-view information as regions’ features, we explicitly model such information into a heterogeneous graph, enabling us to mine different semantics and preserve the heterogeneity of information. This meta-path based graph structure can benefit the crime prediction tasks by improving both model interpretability and predictive performance. On the one hand, as meta-path can explicitly capture semantic relations between regions and complex context features, it can help us make informed decisions and improve the interpretability of the model. On the other hand, compared with random walk based approaches [21, 22], symmetric meta-paths can better capture region-wise similarity conditioned on each specific socioeconomic factor. Besides, compared with approaches that build relation-specific homogeneous graphs [23], the meta-path based framework is more scalable, and is less likely to suffer from the sparsity of observed links between regions. Also, to better capture spatial-temporal dynamics, we cast the meta-path based graph into multiple snapshots, where each snapshot contains learned temporal features from the historical criminal activities indicating the temporal dynamics. By distilling information from the region-to-region paths in each snapshot, we can further combine features from diverse paths.

Furthermore, with the help of the path based attention mechanism, the proposed STMEC framework can obtain weights that suggest the contribution of various paths and further enhance the interpretability of the model. The rationale of designing such meta-path schemas is that the criminal activities of a certain region can be inferred from the region with similar environmental and social structures or from its neighborhoods. For example, when predicting crimes in a downtown area with a higher income level and more diverse populations, apart from the local crime trends, we also believe that another region with similar income level and demographic distribution may share its crime patterns to some extent. In addition, a region is more likely to be crime-prone if its nearby regions are at a higher risk of attracting offenders. Hence, by fusing rich information from the knowledge based graph across the time slots, the framework is able to capture temporal dynamics and retrieve semantics from diverse paths in comparison with existing works.

In summary, we highlight the main contributions of our work as follows:

- We design a new multi-view crime prediction framework STMEC that can expressively capture complex spatial-temporal dependencies, as well as correlations with external factors.
- We explicitly model the interactions between regions and features over time to benefit both the performance and explainability. Furthermore, this new perspective enriches the semantic context within the representations from the graph-structured crime data.
- Extensive evaluations on two real-world datasets collected from New York City (NYC) have been performed, and the results show that STMEC surpasses state-of-the-art baselines in terms of both effectiveness and explainability.

2 Preliminaries

In this section, we begin with some essential definitions and present the problem formulation of crime prediction.

Definition 1 Heterogeneous Information Network. A heterogeneous information network (HIN) is defined as a graph $G = (V, E)$ with multiple entity types and relation types. Each entity $v \in V$ belongs to an entity type \mathcal{A} given by the entity type mapping function $\phi : V \rightarrow \mathcal{A}$, and each edge $e \in E$ belongs to a relation type \mathcal{R} given by the relation type mapping function $\psi : E \rightarrow \mathcal{R}$. By definition we have $|\mathcal{A}| + |\mathcal{R}| > 2$.

In this work, there are 7 entity types representing regions, demographic, income level, job type, commuting ways, urban facility distribution, and geographic information. Given the sandwich structure of meta-path, which is denoted as $\langle \text{region}, \text{factor}, \text{region} \rangle$ in Figure 1, the relation between region and factor is defined as ‘region contains information about factor’. In this work, the HIN is different from the pure region-only graphs, as the entity set contains both regions and attributes (e.g., income level and urban facilities).

Definition 2 Meta-path. A meta-path P in a network is denoted in the form of $A_1 \xrightarrow{R_1} A_2 \xrightarrow{R_2} \dots \xrightarrow{R_l} A_{l+1}$. The composite relation from entity types A_1 to A_{l+1} is described as $R = R_1 \circ R_2 \dots \circ R_l$, where $A_i \in \mathcal{A}, R_j \in \mathcal{R}$.

Definition 3 Meta-path instances. Given a meta-path P of a heterogeneous graph G , a meta-path instance $p \in P$ describes a node sequence from entity v_0 to v_k as $p = \langle v_0, v_1, \dots, v_k \rangle$, where $\forall i, \phi(v_i) = A_i \in \mathcal{A}$, and for each relation $e_i = \langle v_i, v_{i+1} \rangle, \psi(e_i) = R_i \in \mathcal{R}$.

Crime prediction. For each geographic region in a city, we use $\mathcal{Y}_i = \{\mathbf{y}_i^1, \mathbf{y}_i^2, \dots, \mathbf{y}_i^t, \dots, \mathbf{y}_i^T\} \in \mathbb{R}^{T \times C}$ to denote the occurrences of all C crime types (1 for observed and 0 for unobserved) at region r_i during T time slots. Given the region set R , the previous crime records, and the region associated information network G , the objective of this work is to learn a predictive framework which infers whether a certain type of criminal activity will happen in the next time step $T + 1$ at each region $r_i \in I$.

The key notations used in this paper are introduced in Table 1. In this paper, we only consider symmetric meta-paths with the length of 2, denoted as $\langle \text{region}, \text{factor}, \text{region} \rangle$. As shown in Figure 1, the interactions between regions will be modeled by the shared features. For example, region 1 and region 2 are connected as they both belong to high-income area, while region 1 and region 3 will share the information of urbanization as both of them have a large number of urban facilities. Also, region 1, region 4, and region 5 are neighbors to each other, which share the attribute of short distances on the geographic level. The choice of various meta-paths will be further discussed in Section 4.2.

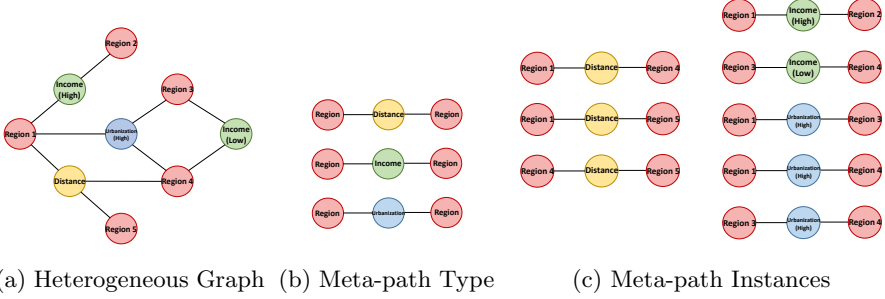


Fig. 1: An illustration of meta-path based crime network. (a) An example of heterogeneous graph consisting of four types of nodes: region, income, urbanization, distance. (b) Three meta-path types in the heterogeneous graph denoted as $\langle \text{region}, \text{factor}, \text{region} \rangle$: $\langle \text{region}, \text{income}, \text{region} \rangle$ (RIR), $\langle \text{region}, \text{urbanization}, \text{region} \rangle$ (RUR), $\langle \text{region}, \text{distance}, \text{region} \rangle$ (RDR). (c) Based on the three meta-path types, all 8 meta-path instances were found from the heterogeneous graph respectively.

Notations	Definitions
G	Heterogeneous information network (HIN)
V	The set of nodes in a graph
E	The set of edges in a graph
v	A node or entity $v \in V$
e	An edge or relation $e \in E$
\mathcal{A}	Type of nodes (entities)
\mathcal{R}	Type of edges (relations)
P	A meta-path
p	A meta-path instance $p \in P$
I	A set of regions
r	A region $r \in I$
\mathbf{W}	Weight matrix
\mathbf{b}	Bias vector
\mathbf{h}	Embedding or hidden state

Table 1: Description of notations used in this paper.

3 Model

In this section, we introduce the proposed model **S**patial-**T**emporal **M**eta-path guided **E**xplainable **C**rime prediction (**STMEC**). STMEC is constructed by four major components: temporal information embedding, meta-path instance encoder, similarity based intra-path aggregation and attention based inter-path aggregation. We first provide an overview of STMEC, and the details of each module are elaborated in the following subsections.

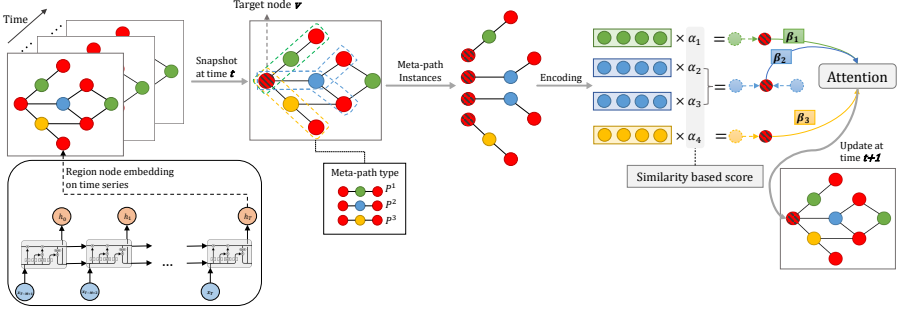


Fig. 2: The architecture of Spatial-Temporal Meta-path Guided Explainable Crime Prediction framework. Here is an example based on three types of meta-paths as denoted in Figure 1. In this example, the red nodes represent regions, while the nodes with other colors are different attributes.

3.1 Overview of STMEC Architecture

The overall architecture of the proposed STMEC model is shown in Figure 2. Different from existing graph based crime prediction models which represent the links between regions by either geographical distance or similarity of points of interest (POI), we model the interaction between regions via an intermediate node of a certain attribute type (e.g., demographic distribution). These interactions are characterized as symmetric meta-paths such as $\langle region, factor, region \rangle$ on a meta-path based graph. Given the temporal properties of this meta-path based graph, the embedding of each region is learned and updated along the time steps. To achieve better representation learning for regions, the procedure is decomposed into four steps. Firstly, the initial embedding of each region is obtained by learning the latent representations of local crime trends with a recurrent neural network (i.e., Long Short-Term Memory networks (LSTM)). Secondly, for each meta-path instance, we integrate the embeddings of attributes and regions along the path. Thirdly, similarity based weights are computed and assigned to meta-path instances to improve the interpretability and accuracy of the model. In this step, the weights are conditioned on the attribute distributions between the pair of regions, and we obtain the representation via weighted aggregation of all meta-path instances of the same type. Finally, the final representation of aggregated meta-paths is generated via an attention mechanism to facilitate predictions. The attention weights help reason out the contributions of different attribute types, providing insights into crime prevention.

3.2 Temporal Information Embedding

We firstly learn the latent representation of each region at every time step from the criminal records. For sequential data modeling, LSTM is known for its ability to capture both short-term and long-term dependencies when compared

with other RNN based models [24]. Thus, in this task, we deploy a time-series oriented LSTM to learn latent representations from the given sequence of crime records.

For each region r_i , given a list of crime records containing T daily data points $\mathcal{Y}_i = \{\mathbf{y}_i^1, \mathbf{y}_i^2, \dots, \mathbf{y}_i^t, \dots, \mathbf{y}_i^T\} \in \mathbb{R}^{T \times C}$, where $\mathbf{y}_i^t \in \mathbb{R}^C$ is the number of crime records for all crime types C at time step t . We aim to initialize the representation of region r_i at time step t based on the crime records from previous M time steps, which is denoted as $\mathcal{Y}_i^M = \{\mathbf{y}_i^{t-M+1}, \dots, \mathbf{y}_i^t\} \in \mathbb{R}^{M \times C}$. By taking a region's features \mathbf{y} at different time steps as the input, the hidden states $\mathbf{h}_{r_i}^t$ derived from the LSTM will be utilized as the initial representation of region r_i at time step t . An LSTM unit is composed of a forget gate, an input gate, and an output gate, which regulate the flow of information. Formally, the LSTM layer performs the following functions to update the hidden states $\mathbf{h}_{r_i}^t$:

$$\begin{aligned}
 \mathbf{f}_{r_i}^t &= \sigma(\mathbf{W}_{xf}\mathbf{y}_i^t + \mathbf{W}_{hf}\mathbf{h}_{r_i}^{t-1} + \mathbf{b}_f) \\
 \mathbf{i}_{r_i}^t &= \sigma(\mathbf{W}_{xi}\mathbf{y}_i^t + \mathbf{W}_{hi}\mathbf{h}_{r_i}^{t-1} + \mathbf{b}_i) \\
 \tilde{\mathbf{c}}_{r_i}^t &= \tanh(\mathbf{W}_{xc}\mathbf{y}_i^t + \mathbf{W}_{hc}\mathbf{h}_{r_i}^{t-1} + \mathbf{b}_c) \\
 \mathbf{o}_{r_i}^t &= \sigma(\mathbf{W}_{xo}\mathbf{y}_i^t + \mathbf{W}_{ho}\mathbf{h}_{r_i}^{t-1} + \mathbf{b}_o) \\
 \mathbf{c}_{r_i}^t &= \mathbf{f}_{r_i}^t \odot \mathbf{c}_{r_i}^{t-1} + \mathbf{i}_{r_i}^t \odot \tilde{\mathbf{c}}_{r_i}^t \\
 \mathbf{h}_{r_i}^t &= \mathbf{o}_{r_i}^t \odot \tanh(\mathbf{c}_{r_i}^t)
 \end{aligned} \tag{1}$$

where \mathbf{y}_i^t is the input at time t with dimension d_y , and $\mathbf{h}_{r_i}^t$ is the hidden state at time t with dimension d_s . Furthermore, the input gate, forget gate, output gate and cell state are denoted as $\mathbf{i}_{r_i}^t$, $\mathbf{f}_{r_i}^t$, $\mathbf{o}_{r_i}^t$, and $\mathbf{c}_{r_i}^t$, respectively. Each of the $\mathbf{W}_{x*} \in \mathbb{R}^{d_y \times d_s}$ is the weight matrix to control information flow from input to LSTM cell, while each of the $\mathbf{W}_{h*} \in \mathbb{R}^{d_s \times d_s}$ is the weight matrix to transform the previous states $\mathbf{h}_{r_i}^{t-1}$ to LSTM cell. Also, $\mathbf{b}_* \in \mathbb{R}^{d_s}$ represents the bias term. The sigmoid function denoted as σ helps the LSTM cell to update or forget the data. For notation simplicity, we denote Eq. 1 as $\mathbf{h}_{r_i}^t = \text{LSTM}(*, \mathbf{c}_{r_i}^{t-1}, \mathbf{h}_{r_i}^{t-1})$ in the following subsections.

3.3 Meta-path Embedding

In crime prediction tasks, external features depicting the community profiles are normally considered as auxiliary knowledge to complement the machine learning methods. For instance, demographics, income level, and human behavioral factors indicating the socioeconomic characteristics [16, 25] are commonly used to improve the crime incident prediction. However, how to leverage heterogeneous and ubiquitous information effectively is always a challenge. In this case, the meta-path based graph is considered to represent heterogeneous information as it can model various relationships between different types of objects intuitively and precisely. Different meta-path based embedding techniques, such as the random-walk based methods [26, 27] (i.e., Metapath2vec and HERec), are proposed to aggregate information from neighbors along the

paths but are generally more focused on the structural information of each meta-path type and simply treat the inherent node attributes as features. However, in the crime prediction context, how the regions correlate and interact with those features are crucial to accurate predictions. In general, criminal activities always interact with different socioeconomic factors, and the relations can be modeled in a symmetric structure denoted as $\langle region, factor, region \rangle$. This structure protects the diversity of auxiliary information and maps the correlation between regions in terms of different views. Thus, inspired by [28], we distill comprehensive semantics by differentiating meta-path instances into different categories and integrating information by meta-path aggregation methods. In this work, we consider six factors as potential causes of crime-prone communities, including demographics, income level, job type, journey to work, urban facilities, and geographical distance. Each factor is represented by a vector that describes the distribution of its attributes. For example, a feature vector for urban facilities carries the proportion of recreation, residential, and public safety facilities.

It is also worth mentioning that, we consider only symmetric meta-paths for capturing region-wise similarity. For example, if two regions have similar income statistics, they will be connected by a virtual meta-path link as $\langle region, income, region \rangle$ (RIR), and it can be extended to RIRIR which has a length of more than 2, but it will reduce the training efficiency as more steps of aggregation are involved. Also, as we focus on learning the importance of different factors to the prediction results, asymmetric meta-path like $\langle region, income, region, job, region \rangle$ (RIRJR) is likely to introduce more noise in the meta-path instance, and will bring difficulties in quantifying the contributions of different socioeconomic factors like income and job in this case. Furthermore, asymmetric meta-paths come with a higher demand on the feature engineering process that heavily depends on domain expertise.

3.4 Meta-path Instance Aggregation

Given target region r_i for which we want to predict the crime incidents in the next time step $t + 1$, we first take the snapshot of the entire meta-path based graph at time t . In the snapshot, we can find a candidate region r_j connects to r_i via an intermediate node indicating a certain factor. As a meta-path is defined by $\langle region, factor, region \rangle$, we denote the meta-path instance as $p(r_i, r_j)$ and the intermediate node as $m^{p(r_i, r_j)}$, where the type of meta-path instance P_A is determined by the type of intermediate node $A \in \mathcal{A}$. For each type of meta-path, the basic idea is to find all meta-path instances containing target node r_i and measure the priority of each instance. This is achieved by quantifying the similarity between the target region and another region w.r.t. their relationships towards the intermediate node. For instance, if region r_i and region r_j both belong to low-income areas, they will be connected by the intermediate node *income*. If r_j has similar measurements regarding the income-related features (i.e., mean, median, and variance in our case), we would consider r_j as an important candidate for predicting events that

happen in r_i when modeling the $\langle \text{region}, \text{income}, \text{region} \rangle$ meta-path. Section 3.4 further introduces the computation of pairwise similarities between two regions in a meta-path instance.

We denote region r_i 's feature vector of a certain factor as \mathbf{m}_{r_i} . For example, the feature vector that describes the region's income level comprises of the median, mean, variance, and stand deviation of the local income. To embed the information along a particular path instance into a low-dimensional vector, we concatenate the node features to preserve the heterogeneity [29, 30]. Following the concatenation, we apply a linear transformation to map the sequence of features into the same latent space. For a meta-path instance $p(r_i, r_j)$, we denote its embedding at time t as follows:

$$\mathbf{h}_{p(r_i, r_j)} = \mathbf{W}_p \cdot \text{CONCAT} \left(\mathbf{h}_{r_i}^t, \mathbf{m}_{r_i}^t, \mathbf{m}_{r_j}^t, \mathbf{h}_{r_j}^t \right) \quad (2)$$

where $\mathbf{h}_{p(r_i, r_j)} \in \mathbb{R}^{d_e}$ is the meta-path instance embedding, and $\mathbf{W}_p \in \mathbb{R}^{d_e \times d'}$ is the learnable parameter. Here, d' is the dimension of the concatenated feature vector and d_e is the embedding size of the concatenated features. In addition, $\mathbf{h}_{r_i}^t$ is the temporal embedding of region r_i learnt from the previous M time steps.

To aggregate information from meta-path instances for target node r_i , we can perform a weighted sum of the instances for each type of meta-path P_A :

$$\mathbf{h}_{r_i}^{P_A} = \sum_{p(r_i, r_*) \in P_A} s(r_i, r_*) \cdot \mathbf{h}_{p(r_i, *)} \quad (3)$$

where r_* denotes the candidate region connected by a meta-path instance belonging to type P_A and ends at region r_i . The similarity score $s(r_i, r_*)$ is computed by our proposed distribution-aware PathSim. In what follows, we present the innovative design of this path based similarity metric.

3.5 Distribution-aware PathSim

PathSim [20] is a well-established method that outstands for its ability to capture the subtle semantic similarities between objects in symmetric meta-paths. The original PathSim is presented below:

$$s'(r_i, r_j) = \frac{2 \times |p_{r_i \rightarrow r_j} : p_{r_i \rightarrow r_j} \in \mathcal{P}|}{|p_{r_i \rightarrow r_i} : p_{r_i \rightarrow r_i} \in \mathcal{P}| + |p_{r_j \rightarrow r_j} : p_{r_j \rightarrow r_j} \in \mathcal{P}|} \quad (4)$$

However, the original PathSim relies only on occurrences of categorical node features and lacks an effective approach to take into account the fine-grained, sub-divided categorical features when computing two regions' similarity in the crime prediction context. For example, in the meta-path with *urban facilities* as the intermediate node, a vector containing proportions of different building facilities has been used to indicate the urbanization level of a region. A

Region	Educational		Recreational	
	Elementary School	High School	Zoo	Pool
r_1	2	2	5	5
r_2	2	2	0	10
r_3	0	0	5	5

Table 2: A toy example to compare the original PathSim and distribution-aware PathSim.

building facility is described as a commonplace that accommodates diverse activities, such as residential, civic, educational, or commercial facilities. These types of facilities are further subdivided into more specific facility types like high school and primary school in the category of educational facilities. Such sub-divided categorical features are commonly observed within the ubiquitous data, making the traditional PathSim incompatible. This is because the similarity between regions w.r.t. different fine-grained categorical features are treated evenly in PathSim, which leads to significant information loss. Hence, we propose a distribution-aware PathSim to complement the similarity metrics. The distribution-aware PathSim $s(r_i, r_j)$ for two regions is given by:

$$s(r_i, r_j) = \sum_{z \in Z} \frac{|z|}{|Z|} \cdot s(r_i, z, r_j) \quad (5)$$

$$s(r_i, z, r_j) = \frac{2 \times |p_{r_i \rightarrow r_j} : p_{r_i \rightarrow r_j} \in \mathcal{P}_z|}{|p_{r_i \rightarrow r_i} : p_{r_i \rightarrow r_i} \in \mathcal{P}_z| + |p_{r_j \rightarrow r_j} : p_{r_j \rightarrow r_j} \in \mathcal{P}_z|}$$

where z represents the facility category (e.g., *Educational*), Z indicates all types of urban facilities, and \mathcal{P}_z denotes the meta-path connected by the category z . Here, $|z|$ and $|Z|$ denote the number of facility types in category z and the number of facility types across all categories. For example, region r_1 in Table 2 has two categories of urban facilities as *Educational* and *Recreational*, where *Elementary School* and *High School* are the 2 facility types of *Educational*, and there are in total 4 facility types: *Elementary School*, *High School*, *Zoo*, and *Pool* across all categories. Thus, $\frac{|z|}{|Z|}$ can represent the proportion of *Educational* in all facility types as $\frac{2}{4}$. Also, $s(r_i, z, r_j)$ represents the similarity score between region r_i and r_j in terms of the category z , while $s(r_i, r_j)$ is the similarity between two regions concerning all categories Z . The measurement is mainly based on the number of path instances between two regions, which is denoted as $|p_{r_i \rightarrow r_j}|$.

To demonstrate how our proposed method works, we use a toy example as shown in Table 2 to illustrate the reliability of the method compared with the original PathSim. The example shows the number of urban facilities in region r_1 , r_2 , and r_3 . The urban facilities can be divided into two categories as *Educational* and *Recreational*, and each has two facility types as

Elementary School and *High School*, *Zoo* and *Pool* respectively. We aim to find the region with the most similar structure as r_1 . As r_2 has both educational and recreational facilities of the same amount, it is more close to the urban structure as r_1 . PathSim measures the similarity scores as: $s'(r_1, r_2) = \frac{2 \times (2 \times 2 + 2 \times 2 + 5 \times 10)}{(2 \times 2 + 2 \times 2 + 5 \times 5) + (2 \times 2 + 2 \times 2 + 10 \times 10)} = 0.699$, while $s'(r_1, r_3) = 0.926$. The distribution-aware PathSim complements the problem by taking the weighted sum of PathSim in terms of categories. Thus, we compute the similarity score as $s(r_1, r_2) = \frac{2}{4} \cdot 1 + \frac{2}{4} \cdot \frac{2 \times (5 \times 10)}{(5 \times 5 + 5 \times 5) + (10 \times 10)} = 0.833$, while $s(r_1, r_3) = 0.5$. Apparently, our distribution-aware PathSim has stronger consistency with human intuition owing to the consideration of different categories.

3.6 Attention for Meta-path based Context

Intuitively, different meta-paths carry different semantics in a region-region interaction. In the task of crime prediction, it is hard to identify the leading factor that contributes more to criminal behaviors. Also, for different regions, a meta-path may have varying semantics as it collects information from different instances via the interaction. Hence, we apply a graph attention layer to rank the importance of meta-paths and then summarize the flow of information by weighted sum.

For region $r_i \in I$, we have the summarization of the meta-path P_A denoted as $\mathbf{h}_{r_i}^{P_A}$, where $P_A \in \mathcal{P}$ and \mathcal{P} is a set of meta-paths containing node r_i . First, we transform the meta-path based representations for all nodes $r_i \in I$, and obtain the average value with respect to each meta-path type P_A :

$$\mathbf{u}^{P_A} = \frac{\sum_{r_i \in I} \tanh(\mathbf{M}_u \cdot \mathbf{h}_{r_i}^{P_A} + \mathbf{b}_u)}{l} \quad (6)$$

where $\mathbf{M}_u \in \mathbb{R}^{d_a \times d_e}$ and $\mathbf{b}_u \in \mathbb{R}^{d_a}$ are learnable parameters. The number of nodes is denoted by l .

Then the attention mechanism is utilized to fuse the meta-path based context, the weights are learnt over different types of meta-path as follows:

$$\begin{aligned} e^{P_A} &= \mathbf{q}^T \cdot \mathbf{u}^{P_A} \\ \beta^{P_A} &= \frac{\exp(e^{P_A})}{\sum_{P_A \in \mathcal{P}} \exp(e^{P_A})} \\ \mathbf{h}_{r_i}^{\mathcal{P}} &= \sum_{P_A \in \mathcal{P}} \beta^{P_A} \cdot \mathbf{h}_{r_i}^{P_A} \end{aligned} \quad (7)$$

where $\mathbf{q} \in \mathbb{R}^{d_a}$ is the attention vector to be learned in the training process, and β^{P_A} is the learnt importance score of meta-path P_A . The summarized context information based on each type of meta-path is embedded as $\mathbf{h}_{r_i}^{\mathcal{P}}$, which will be projected to a C -dimensional output via a dense layer with sigmoid activation. The final output is the estimated probability of crime c that will happen in region r_i , which is denoted as $\hat{y}_{r_i}^{t,c}$.

3.7 Training

Our objective is to obtain the value of $\hat{\mathbf{y}}_{r_i}^t$ at each time step t , where the c -th element $\hat{y}_{r_i}^{t,c}$ denotes the probability that crime event of category c will happen in the next time step $t + 1$. As this can be viewed as C binary classification tasks, we employ cross entropy as the loss function:

$$\mathcal{L} = - \sum_{(r_i, c, t) \in S} y_{r_i}^{t+1, c} \log \hat{y}_{r_i}^{t, c} + (1 - y_{r_i}^{t+1, c}) \log (1 - \hat{y}_{r_i}^{t, c}) \quad (8)$$

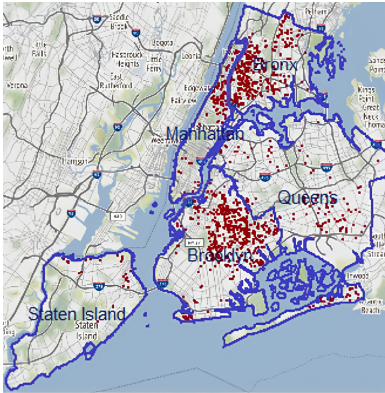
where $\hat{y}_{r_i}^{t, c}$ is the estimated probability of crime c that will happen in region r_i in the next time slot $t + 1$ and $y_{r_i}^{t+1, c}$ is the corresponding ground-truth record at time slot $t + 1$. Also, S is the crime event set in the training process. In this work, the model parameters are learnt by minimizing the loss function with Adaptive Moment Estimation (Adam) [31].

4 Experiment

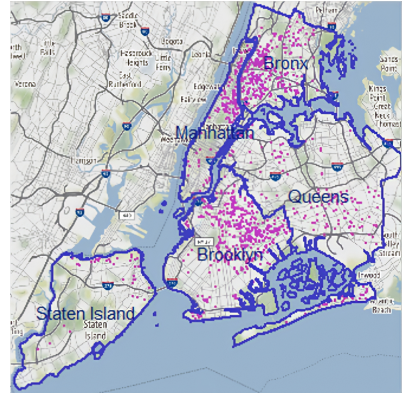
4.1 Experiment Settings

4.1.1 Datasets

We integrate multiple public datasets from various resources in New York City (NYC). The performance of our framework is evaluated via the datasets collected from both 2014 and 2015.



(a) Gun Violence 2014



(b) Gun Violence 2015

Fig. 3: Gun Violence Distribution in NYC.

(1) **Census Data** [32]: There are 2161 records of census tracts in the 2015 American Community Survey containing information about population, commuting ways, job type, and income level.

(2) **Points of Interest (POI)** [33]: We collect more than 15,000 records of commonplaces, which includes 13 facility domains like Residential Places, Education Facility, Cultural Facility, Recreational Facility, Social Services Facilities. After allocating the number of data points to the corresponding region by each type, the distribution of points in each region can reflect the level of urbanization.

(3) **Crime Data** [34]: We evaluate the STMEC model on the crime data collected from Jan 1, 2014, to Dec 31, 2015 (2*365 days) in NYC. For the prediction tasks, we select the top 10 most common crimes. Apart from this, we also investigate the dangerous weapon related crimes, as more than 200 people in the United States are wounded or killed by gun violence every day [35]. As shown in Figure 3, gun violence in NYC usually happens in Brooklyn and the borders of Manhattan and Bronx, which indicates that gun violence is highly related to geographical locations.

There are in total 71 districts in NYC based on the partition rule that is valid from 2013 to 2020, and our experiments are conducted on the district level. Hence, the ubiquitous data has been integrated into each district to represent a higher level of various characteristics. The statistics of crime data and POI are shown in Table 3 and Table 4.

Data Source	Category	Avg. Days with Crimes		Avg. Days without Crimes	
		2014	2015	2014	2015
NYC Crime Reports 2014 and 2015	Petite Larceny	296	294	69	71
	Harassment	281	281	84	84
	Assault	258	258	107	107
	Criminal Mischief	254	256	111	109
	Grand Larceny	250	249	115	116
	Dangerous Drugs	167	154	198	211
	Against Public Order	173	182	192	183
	Felony Assault	165	165	200	200
	Robbery	152	155	213	210
	Burglary	155	146	210	219
	Dangerous Weapons	106	105	259	260

Table 3: Data statistics of crime records: average days with and without crimes across all regions.

Data Source	Category	#(2014)	#(2015)	Category	#(2014)	#(2015)
NYC POI 2014 and 2015	Commercial	711	724	Cultural	520	522
	Education	3037	3472	Government	662	723
	Health Services	215	220	Miscellaneous	648	651
	Public Safety	592	596	Recreational	2458	2481
	Religious	1164	1201	Residential	2930	2967
	Social Services	1395	1409	Transportation	455	542
	Water	281	281			

Table 4: Data statistics of POI: number of POI of different categories in NYC 2014 and 2015.

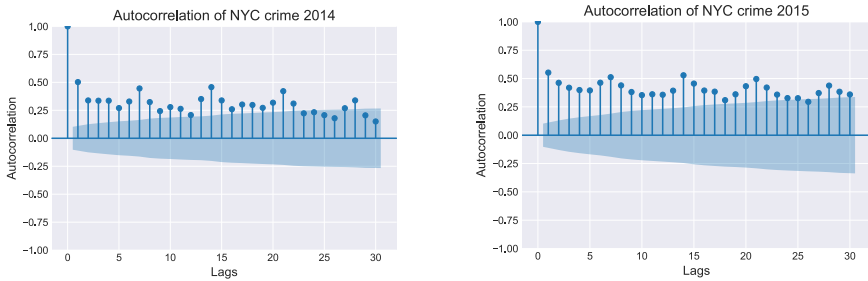


Fig. 4: ACF plot of crime trends in 2014 and 2015.

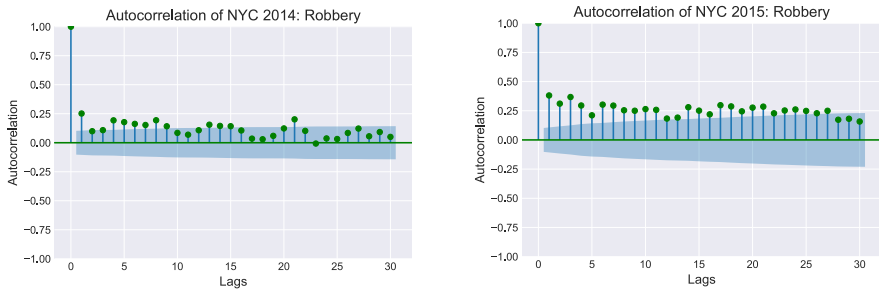


Fig. 5: ACF plot of robbery trends in 2014 and 2015.

4.1.2 Analysis on Crime Trends

To better understand the crime trends, we explore the correlation between the crime events and their own lags by using the Autocorrelation Function (ACF). Fig. 4 shows the non-stationary characteristics of both crime trends, given the slowly decreasing autocorrelation values along the lags. Additionally, the plot also indicates different temporal dependencies on historical crimes across two datasets, as the autocorrelations of different datasets show different levels of sensitivity to their lags. Specifically, compared with crime trends in 2014, crime

trends in 2015 show a stronger correlation (i.e., a larger autocorrelation value of recent lags) between the current and recent records.

Furthermore, the difference of temporal dependencies among two datasets is also observed from fine-grained crime types. For example, in Fig.5, robbery trends of NYC 2014 spikes at lag 21, indicating a strong correlation between the current crime events and the one happened 21 days before, while a weak correlation is observed between the current crime events and recent lags (lag 2 and lag 3). However, robbery trends of 2015 show a stronger temporal dependency across 4 weeks' lags. As we will further discuss in Section 4.5.1, these findings suggest different model sensitivity to varying time window sizes in different datasets.

4.1.3 Evaluations

As an evaluation of the stability and reliability of model performance for different datasets, the experiments are done for crime events in 2014 and 2015 respectively. To ensure the consistency of training and test for STMEC and all baseline models, all prediction tasks start from 29th Jan of each year, and the data is split into 75% (255 days) for training, 5% (18 days) for validation, and 20% (64 days) for test. The choice of the commencement date is based on the optional time window used for crime prediction tasks. To compare STMEC with state-of-the-art baselines, we use four types of evaluation metrics to fully investigate the performance of each model on the test set:

- (1) **Macro-F1 and Micro-F1 score**: To measure the performance of the model across different categories (i.e., Robbery and Grand Larceny) of crime events, we utilize Macro-F1 and Micro-F1 [36]. Models with better overall performance usually have higher Micro-F1 and Macro-F1 scores.
- (2) **Macro-Recall and Micro-Recall score**: Considering that criminal activities can lead to an immeasurable loss to the society, the ideal predictor is supposed to minimize the number of false negatives, that is, we want to correctly identify as many risky activities as possible. Thus, the score of recall is a crucial metric in crime prediction. Similar to Macro and Micro F1 score, the Macro and Micro Recall [37] is computed by averaging the performance across different categories.
- (3) **F1 score**: F1 score is used to measure the prediction accuracy of the model for an individual category of crime, which computes the harmonic mean of precision and recall.
- (4) **Recall**: Recall is used to evaluate the performance of the model for a single category of crime events, which suggests the ability to correctly identify the crime events that truly happened.

4.1.4 Baselines

The performance of the proposed model will be compared with the state-of-the-art baseline models. Most of the Graph Convolutional Networks (GCN) based models are inherited from the task of traffic prediction, which is also used

for predicting crime events in some studies [38–40]. Thus, we will compare the performance of our model with these outstanding models, given the purpose of crime prediction is also to capture the spatial and temporal dependence. Please note that we use the same input data including geographic, demographic, and urban-related information for all baseline models but with different data representations concerning different architectures of baseline models.

We briefly introduce the baseline methods for comparison below:

- **Multilayer Perceptron (MLP)**: This is the conventional neural network with 3 dense layers to learn the representations from given features.
- **GCN** [41]: This neural network learns the features by aggregating information from neighboring nodes. To test the performance of this model, the input data has been organized into a graph structure where the nodes represent each region, while the edges are given by the distance between the adjacent regions.
- **TGCN** [42]: This model is normally employed to capture the spatial and temporal dependence simultaneously. It is a joint framework with the GCN and gated recurrent unit (GRU).
- **LSTM-GCN** [43]: This model is quite similar to TGCN. Instead of using GRU to capture the temporal pattern, this model replaces the component with LSTM unit.
- **STGCN** [44]: This model is a typical spatial-temporal model but with complete convolutional structures. It can also capture comprehensive spatial-temporal dependence.
- **MiST** [9]: MiST is a attention based recurrent framework for crime prediction. It surpasses traditional regression based models (i.e., SVR and ARIMA) as well as several state-of-the-art deep learning models. Thus, MiST is a strong baseline to evaluate and performance of our proposed model.
- **HAGEN** [45]: HAGEN is the most recent graph neural network specifically designed for crime forecasts. This framework captures the crime correlation between regions via distance based and context based (e.g., POI) similarities.
- **GSNet** [23]: GSNet is a homogeneous graph based framework which models different kinds of spatial correlations by different types of context features (e.g., POI similarity, geographical similarity). Based on our problem setting, we have deployed this framework by constructing six homogeneous graphs which correspond to the six factors explored in this paper.

4.2 Parameter Settings

In our work, the hyperparameters of each baseline model are carefully tuned to ensure optimal results. We implement STMEC with Pytorch architecture. We set the dimension of temporal embedding d_s as 128 and the number of LSTM layers as 2. The optimal time window M , from which the temporal dynamics are learned, is set as 28 days for 2015 dataset and 21 days for 2014 dataset. Also, The embedding size of meta-path instances d_e is set as 64 and

the attention vector size d_a is set as 128. Additionally, the learning process is optimized by Adam, with the learning rate 0.0001. The effect of different hyperparameter setting has been discussed in Section 4.5.

We investigate 6 different types of factors that may affect the criminal activities which are represented as meta-paths: $\langle \text{region}, \text{demographic}, \text{region} \rangle$ (RDR), $\langle \text{region}, \text{income}, \text{region} \rangle$ (RIR), $\langle \text{region}, \text{job type}, \text{region} \rangle$ (RJR), $\langle \text{region}, \text{commuting ways}, \text{region} \rangle$ (RCR), $\langle \text{region}, \text{urbanization}, \text{region} \rangle$ (RUR), and $\langle \text{region}, \text{geographic}, \text{region} \rangle$ (RGR). The importance of the factors is discussed in the following subsections.

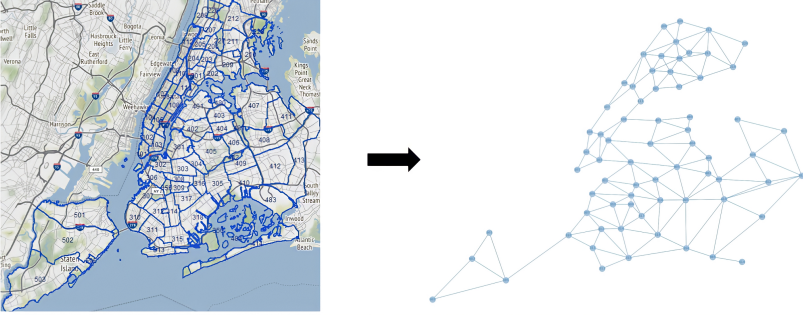


Fig. 6: Data representation in GCN based model. Each node represents a region (district) with integrated features (i.e., demographics and urban structures), and the adjacent regions are connected by edges which indicate the distance in between.

4.3 Model Performance Comparison

4.3.1 Overall Performance across All Crime Types

As shown in Table 5, the proposed model STMEC outperforms all existing state-of-the-art deep learning models by achieving the best scores across all evaluation metrics. In the dataset from NYC 2015, we improve 2%, 6%, 8.2%, 5.7% of the crime prediction framework MiST with respect to Macro-F1, Micro-F1, Macro-Recall, and Micro-Recall scores. Also, our model shows competitive performance even compared to the most recent spatial-temporal frameworks HAGEN and GSNet. The advantages of our proposed model persist on the other dataset from 2014 as well. The results prove that our model benefits with better performance by explicitly modeling the interactions between crime events and the possible causes. By comparing the performance of MLP and GCN which ignore the long-term temporal dynamics, no obvious loss of the performance is observed. This result suggests that the crime events in general are largely affected by the most recent trends. Also, the slight improvement of GCN as compared to MLP indicates the importance of geographical factors, as the GCN based model constructs the data as geographic based graphs, which are shown in Figure 6. Consistent with the findings of temporal impacts on crime events, the rest of GRU or LSTM based models

Datasets	Metrics	MLP	GCN	TGCN	LSTM-GCN	STGCN	MiST	HAGEN	GSNet	STMEC
NYC 2014	Macro-F1	0.794	0.802	0.803	0.792	0.803	0.797	0.816	0.813	0.816
	Micro-F1	0.707	0.724	0.732	0.721	0.733	0.719	0.761	0.759	0.764
	Macro-Recall	0.688	0.713	0.738	0.715	0.733	0.724	0.786	0.786	0.791
	Micro-Recall	0.768	0.792	0.807	0.785	0.803	0.797	0.846	0.844	0.849
NYC 2015	Macro-F1	0.793	0.798	0.784	0.793	0.795	0.796	0.813	0.810	0.816
	Micro-F1	0.715	0.716	0.690	0.722	0.710	0.703	0.756	0.748	0.763
	Macro-Recall	0.688	0.699	0.667	0.714	0.699	0.707	0.778	0.768	0.789
	Micro-Recall	0.763	0.777	0.752	0.786	0.780	0.789	0.839	0.834	0.846

Table 5: Performance comparison with baselines.

which focus more on sequential information cannot significantly improve the performance with comparison to conventional neural networks.

4.3.2 Performance on Individual Crime Type

Additionally, we explore the effectiveness of STMEC in forecasting each category of crime events. From Figure 7, we observe that for frequent crime events (from (a) **Petit Larceny** to (e) **Grand Larceny**), most of the deep learning baselines can persist remarkable performances while STMEC stays competitive for predicting those kinds of crimes. However, for crime events that rarely happen (from (f) **Dangerous Drugs** to (k) **Dangerous Weapons**), most of the baselines fail to capture the dynamic patterns and undermine the ability to identify the occurrence of criminal activities. Although STMEC falls slightly behind HAGEN and GSNet in predicting crimes related to against public order and felony assault, it alleviates the scarcity of other rarer crime types by achieving 5%-20% higher recall and 3%-10% higher F1 score. For instance, when predicting dangerous drugs related crimes in 2015, STMEC achieves recall of 0.744 and F1 score of 0.72. It outperforms the second-best baseline model GSNet which achieves recall of 0.644 and F1 score of 0.685. Furthermore, STMEC achieves the highest recall and F1 score of predicting burglary in 2014, which are 0.627 and 0.615 respectively. This result reveals 6.7% and 4.3% improvement in terms of recall and F1 score compared to the best baseline HAGEN. Given the significant improvement in predicting uncommon crimes, we can conclude that the performance of STMEC is stable and robust across different crime types.

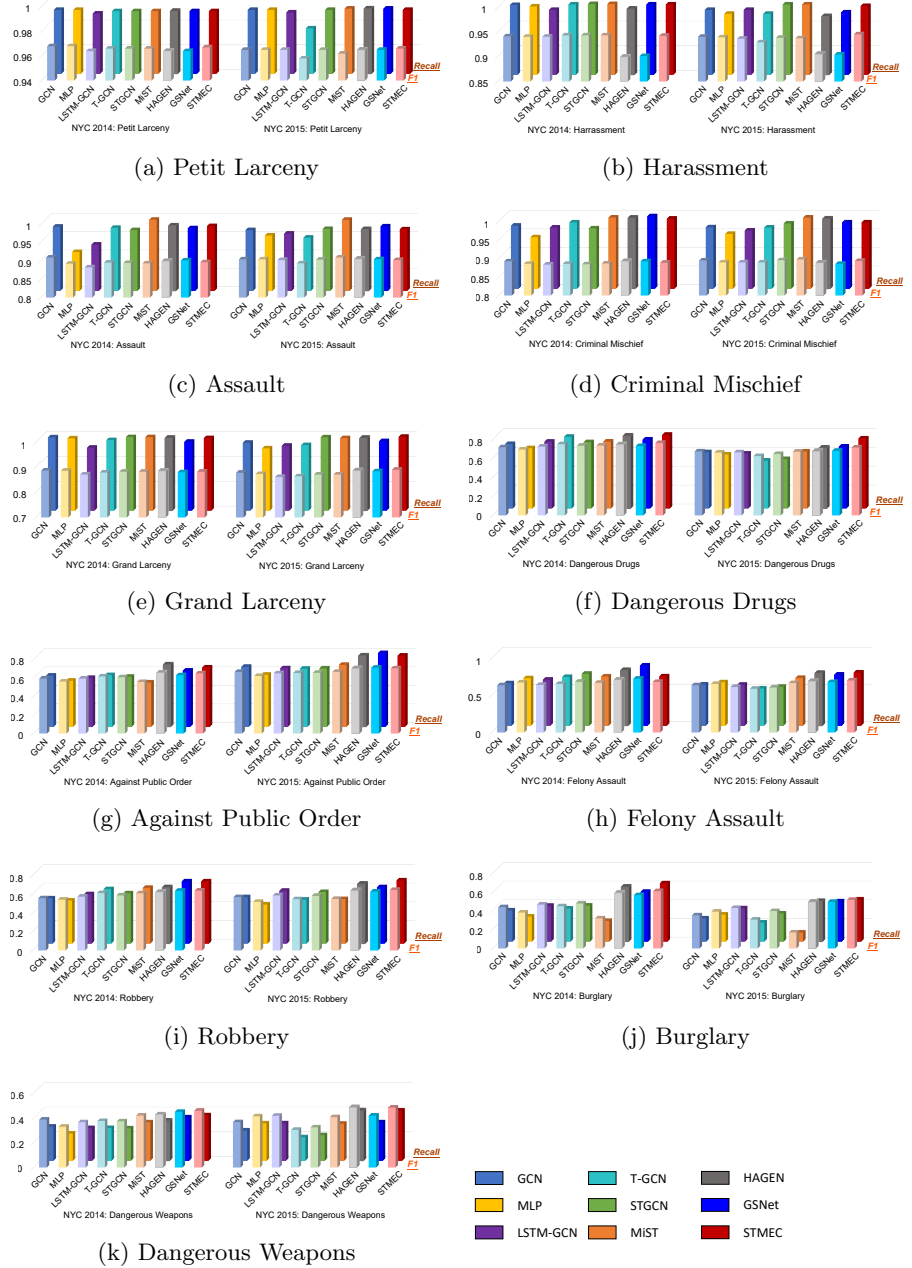


Fig. 7: Performance comparison by each type of crime events.

Factors	Mean	Min.	Median	Max.
Demographics	0.167	0.049	0.157	0.359
Income	0.177	0.104	0.164	0.375
Job	0.00019	0.00012	0.00018	0.00027
Commuting	0.112	0.004	0.085	0.459
Urbanization	0.502	0.167	0.513	0.744
Geographic	0.040	0.012	0.037	0.078

Table 6: Summary table of importance score obtained from attention.

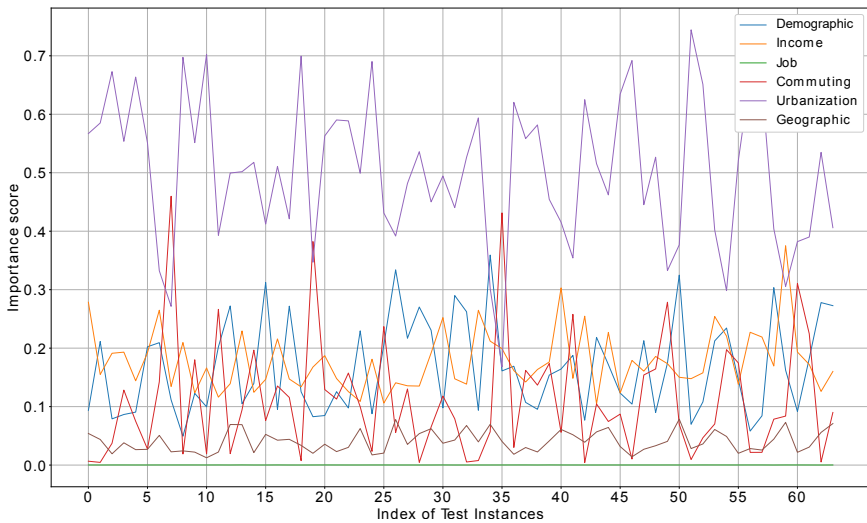
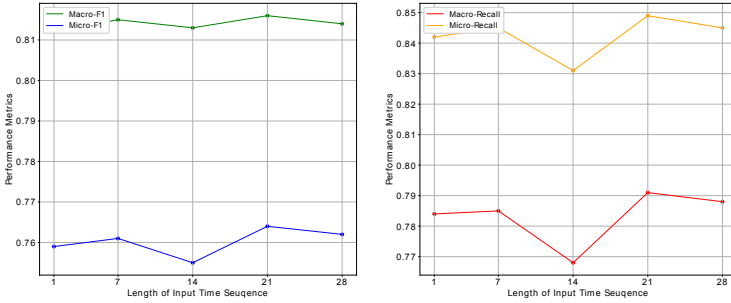


Fig. 8: Variations of attention scores in testset (NYC 2014).

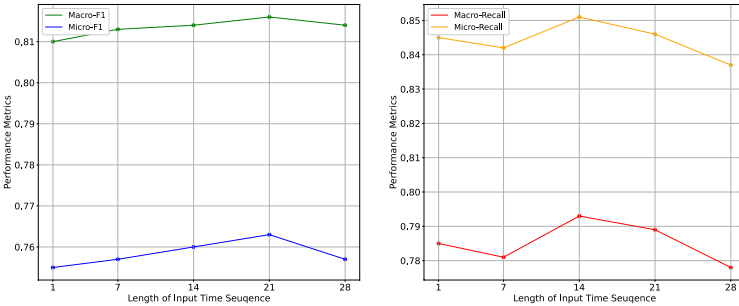
4.4 Analysis of Explainability

Apart from the superior performance given by STMEC, another contribution of the framework is to give explanations on forecasts. This work involves 6 different types of meta-paths which represent the features from different categories of potential factors. As we generate pre-defined region-to-region instances and sum up the impacts from each path by a given similarity score, the effect of the black box is relieved by explicitly modeling the interactions and ranking priorities of the path instances. Furthermore, the attention mechanism that obtains the weight of each meta-path type also helps to rank the

importance of factors in the crime prediction tasks. Table 6 demonstrates the summary of importance scores with respect to different factors. As the scores are obtained from each test instance given by day, the result indicates that the importance of each factor varies a lot along the timeline. Specifically, we can observe the variation of importance for each factor from Figure 8. It shows that urbanization level is the leading factor for most of our predictions, while the type of job in the population is the least important factor in the task. Additionally, we can also observe that the impact of geographical information is relatively stable, while the others dramatically change up and down. It is worth noticing that the causes of criminal activities are not constant along the time. This observation supports our idea of constructing the model by considering the variations and interactions between features.

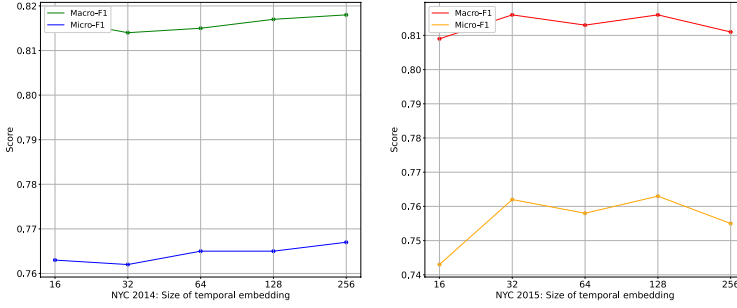


(a) NYC 2014.

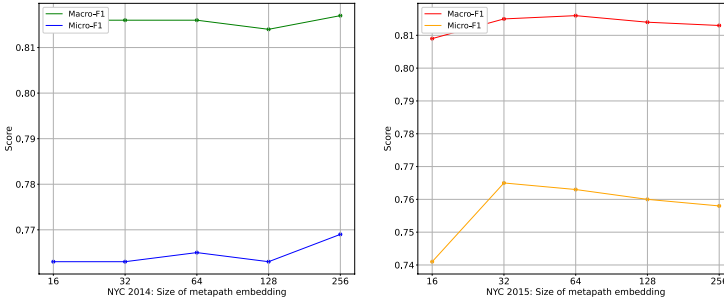


(b) NYC 2015.

Fig. 9: Performance of model across different time window sizes.



(a) Impact of temporal embedding.



(b) Impact of meta-path embedding.

Fig. 10: Impact of embedding size.

4.5 Hyperparameter Study

4.5.1 Effect of the Temporal Scale

Since the crime prediction is conducted by utilizing the last M days of Observations, the length of the encoded time-series sequence is one of the most essential parameters to assist in capturing the temporal dynamics. However, as we observed in Section 4.3.1, the experimental results reveal that the difference between encoding short-term time dependency (one day) and long-term time dependency (up to 4 weeks) is not significant. To further justify this observation and choose the optimal size of the time window for our proposed model, we investigate the change of performance across different length of input sequence M . Figure 9 depicts the performance of STMEC changes across different choice of time window M . As we can observe from the figure, for dataset NYC 2014, the performance of STMEC becomes better as the size of the time window M increases, but saturates when M reaches 21. Also, as we further analyze the impact of time window for NYC 2015 in Figure 9b, the experimental results suggest that the optimal window size that achieves the highest F1 score is still 21, but the model obtains better recall when we set the window size to 14. Thus, based on different patterns shown in different datasets, we

can infer that the change of performance under different time window settings is mainly due to the specific periodicity of crime trends in the datasets. The result is consistent with the observation in Section 4.3.1. As the experimental results in Section 4.3.1 suggest, the crime trends of NYC 2015 tend to have more temporal patterns in the short term, which benefits MLP and GCN that only use features from one step earlier and weakens TGCN that will possibly capture the noise from long-term data. The ACF plots in Fig.4 support our observation, as the recent lags of crime trends in 2015 have larger correlation values compared with crime trends in 2014. By choosing the optimal size of the time window, the performance of the model is slightly improved even compared to the worst option that set the size of the time window to 1. Hence, the crime events are not as temporal-correlated as we thought, and we can barely improve the crime prediction tasks more by solely investigating the temporal features.

4.5.2 Effect of the Embedding Size

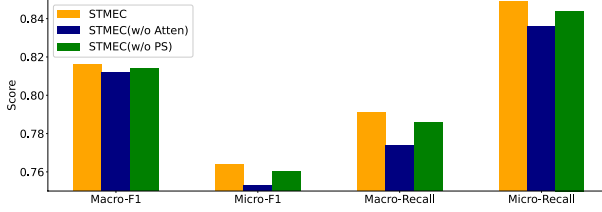
To understand the effect of different embedding size, we further examine the size of temporal embedding in LSTM component, and the size of meta-path embedding during node aggregation. As shown in Figure 10a and Figure 10b, when the size of temporal embedding is set to 128 and the size of meta-path embedding is set to 64, the model can achieve slightly better F1 scores as compared to the others. However, as the difference between F1 scores is only around 1%, we can conclude that our model is insensitive to the size of latent representations.

4.6 Ablation Study

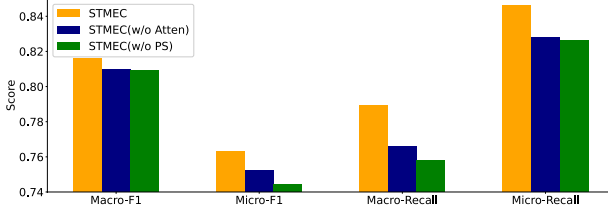
To understand the significance of different components in our proposed framework, we further examine the efficacy of the attention module and the distribution-aware PathSim by replacing them with a mean aggregator in the degraded variants of STMEC. In general, the experimental results in Figure 11 have shown that both key components are beneficial to the performance of our model. Besides, attention module reflects more significance on predicting crimes of NYC 2014, while PathSim shows more potential in predicting crimes of NYC 2015.

5 Related Work

Urban mobility dynamics. Apart from investigating ubiquitous data and historical crime records over time, some studies also analyze the influence of urban mobility dynamics on crime events [12, 46–50]. [47] proposed the User Associated Dynamic Crime Risk (UADCR) features to associate human movement and the risk of a region that may involve in crime events. Based on this work, [48] built a directed weighted graph to analyze the relationship between crime rate and human movements in different periods of the



(a) NYC 2014.



(b) NYC 2015.

Fig. 11: Significance of different component in STMEC.

day. Apart from this, [49] also crafts the spatial-temporal features of human activities from social networks and transportation data, and compared the performance between conventional methods and the tree based machine learning techniques.

Semantic representation learning. As spatial and temporal patterns from human mobility reveal the underlying causes of criminal behaviors, the semantics behind the activity patterns are also discussed in some work [51, 52]. Semantic representation learning can strengthen the understanding of the urban dynamics and issues in various tasks, such as crime, traffic, and user demographics in urban regions. SUME [53] learns a semantic-enhanced embedding of the heterogeneous network which has various types of nodes and edges to infer user demographics. Although this framework is set to optimize user profiles, the implicit representation of urban regions is also learned throughout the task, which sheds light on the possibilities that such similarity based measurements can also help deal with region-level crime prediction tasks. Regarding the semantic learning in crime predictions, one most recent work [51] handles dynamic chain effect and multidimensional features for performing multi-incident co-prediction. This work explicitly exploits the behind-the-scenes chain-like triggering mechanism and tackles the challenging problem caused by incident sparsity. Further more, to learn embeddings from social networks, LBSN2Vec++ [54] is proposed to preserve the information of social relationships and user mobility by encoding friendship edges between users and category hyperedges across different node domains.

Spatial-temporal modelling. There are also plenty of recent studies that mine the spatial-temporal dependencies for other stochastic systems, such as human trajectory [55, 56], e-commerce [57, 58], social network [59, 60] and water quality [61]. Most of the recent methods are deep learning based models and well capture spatial-temporal dependencies with respect to the particularity of certain tasks. For example, [55] proposes a graph attention based sequence-to-sequence model to predict crowd trajectories. Considering that human motion is continuous and forward-looking, the framework explicitly models the continuity of interactions among pedestrians. Additionally, [61] utilizes transfer learning to aggregate information from multiple cities and captures long-term periodicity by a pattern based spatial-temporal memory. Further more, the traffic accident prediction framework GSNet [23] models different kinds of spatial correlations by different types of context features. However, using separate homogeneous graphs inevitably incurs sparse connections between region nodes as there is only one relation type considered. Different to existing spatial-temporal models, our proposed method can learn high-quality region embeddings by utilizing meta-paths in a unified HIN, which allows for simultaneously learning the importance of different factors towards the prediction results.

Crime prediction. Although most of the existing work aims to predict the occurrence of criminal activities, the analysis of more specific factors (e.g., income level) is left untouched in deep learning based models. Unlike traditional regression models where the coefficients directly indicate the importance of features [62], it is still a challenge to explain the feature importance in state-of-the-art deep methods for crime prediction. Also, while some work [62–64] has widely explored the demographics, POIs, and geographical features in crime prediction tasks, our model novelly depicts the relations between regions by different socioeconomic factors, and its performance and explainability are strengthened via the path-enriched features in the graph-structured data. In addition to exploring spatial-temporal impacts on criminal events, some studies [9, 45, 65] also include the cross-type correlations of urban crimes to enhance the accuracy of crime prediction. CCC [65] jointly captures the intrinsic correlations between crime types and the spatial-temporal correlations of criminal activities by mathematical modeling. As our proposed model focus more on the impact of different socioeconomic factors on the occurrence of different crimes, there is potential to further capture correlations between different crime types in our future work.

6 Conclusion

In this paper, we propose a novel framework STMEC which explicitly models the dynamic interactions between regions over time with knowledge-aware paths from multiple views. We also explore the contribution of different factors that potentially result in criminal activities with attention mechanism. The experiments from two real-world crime events datasets show that the proposed

framework outperforms state-of-the-art baselines on key metrics of performance and explainability. Future work may include the following directions: 1) Integrate the impact of urban mobility/human activities, and 2) Explore the importance score of different factors of each specific region.

7 Statements and Declarations

7.1 Ethical Approval and Consent to participate

This work has been reviewed by the Research Ethics and Integrity and is deemed to be exempt from ethics review under the National Statement on Ethical Conduct in Human Research and relevant University of Queensland policy (PPL 4.20.07).

7.2 Human and Animal Ethics

This article does not contain any experimentation with human or animal subjects.

7.3 Consent for Publication

Not applicable.

7.4 Availability of Supporting Data

All datasets used for supporting the conclusions of this article are available from the public data repository at the website of data.cityofnewyork.us and www.kaggle.com.

7.5 Competing Interests

All authors have no competing interests as defined by Springer, or other interests that might be perceived to influence the results and/or discussion reported in this paper.

7.6 Funding

No funding was received for conducting this study.

7.7 Authors' Contributions

Yuting Sun implemented the methodology, performed data curation, wrote the original draft, and conducted the experiment.

Tong Chen proposed the conceptualization and methodology, prepared the figures, and performed review and editing.

Hongzhi Yin proposed the research problem and methodology, supervised the whole research work, wrote the introduction and abstract parts, and performed review and editing.

7.8 Acknowledgements

We gratefully thank Dr. Thomas Taimre (the University of Queensland) and Dr. Radislav Vaisman (the University of Queensland) for valuable discussions on this research and helpful comments on the manuscript. This work is supported by Australian Research Council Future Fellowship (Grant No. FT210100624) and Discovery Project (Grant No.DP190101985).

7.9 Authors' Information

Yuting Sun, Ph.d candidature, School of Information Technology and Electrical Engineering, the University of Queensland, Brisbane, Australia.

Tong Chen, Lecturer, School of Information Technology and Electrical Engineering, the University of Queensland, Brisbane, Australia.

Hongzhi Yin, Associate Professor/ARC Future Fellow, School of Information Technology and Electrical Engineering, the University of Queensland, Brisbane, Australia.

References

- [1] GBD 2017 Causes of Death Collaborators: Global, regional, and national age-sex-specific mortality for 282 causes of death in 195 countries and territories, 1980–2017: a systematic analysis for the global burden of disease study 2017. *The Lancet* **392**(10159), 1736–1788 (2018). [https://doi.org/10.1016/S0140-6736\(18\)32203-7](https://doi.org/10.1016/S0140-6736(18)32203-7)
- [2] Russell, S.: Estimating the costs of serious and organised crime in australia 2016–17. Statistical Report 9, Australian Institute of Criminology, Canberra (October 2018)
- [3] de Melo, S.N., Pereira, D.V.S., Andresen, M.A.: Spatial-temporal variations of crime: A routine activity theory perspective. *International Journal of Offender Therapy and Comparative Criminology* **62**(7), 1967–1991 (2017). <https://doi.org/10.1177/0306624X17703654>
- [4] Li, Z., Zhang, T., Yuan, Z., Wu, Z., Du, Z.: Spatio-temporal pattern analysis and prediction for urban crime. In: 2018 Sixth International Conference on Advanced Cloud and Big Data (CBD), pp. 177–182 (2018). <https://doi.org/10.1109/CBD.2018.00040>
- [5] Nafi'iyah, N., Mauladi, K.F.: Linear regression analysis and svr in predicting motor vehicle theft. In: 2021 International Seminar on Application for Technology of Information and Communication (iSemantic), pp. 54–58 (2021). <https://doi.org/10.1109/iSemantic52711.2021.9573225>
- [6] Zhao, X., Tang, J.: Modeling temporal-spatial correlations for crime

- prediction. In: Proceedings of the 2017 ACM on Conference on Information and Knowledge Management. CIKM '17, pp. 497–506 (2017). <https://doi.org/10.1145/3132847.3133024>
- [7] Yi, F., Yu, Z., Zhuang, F., Zhang, X., Xiong, H.: An integrated model for crime prediction using temporal and spatial factors. In: 2018 IEEE International Conference on Data Mining (ICDM), pp. 1386–1391 (2018). <https://doi.org/10.1109/ICDM.2018.00190>
- [8] Huang, C., Zhang, J., Zheng, Y., Chawla, N.V.: Deepcrime: Attentive hierarchical recurrent networks for crime prediction. In: Proceedings of the 27th ACM International Conference on Information and Knowledge Management. CIKM '18, pp. 1423–1432 (2018). <https://doi.org/10.1145/3269206.3271793>
- [9] Huang, C., Zhang, C., Zhao, J., Wu, X., Yin, D., Chawla, N.: Mist: A multiview and multimodal spatial-temporal learning framework for citywide abnormal event forecasting. In: The World Wide Web Conference. WWW '19, pp. 717–728 (2019). <https://doi.org/10.1145/3308558.3313730>
- [10] Snaphaan, T., Hardyns, W.: Environmental criminology in the big data era. *European Journal of Criminology* **18**(5), 713–734 (2021). <https://doi.org/10.1177/1477370819877753>
- [11] Chen, H., Yin, H., Sun, X., Chen, T., Gabrys, B., Musial, K.: Multi-level graph convolutional networks for cross-platform anchor link prediction. In: Proceedings of the 26th ACM SIGKDD International Conference on Knowledge Discovery & Data Mining. KDD '20, pp. 1503–1511 (2020). <https://doi.org/10.1145/3394486.3403201>
- [12] Wang, Y., Ge, L., Li, S., Chang, F.: Deep temporal multi-graph convolutional network for crime prediction. In: Conceptual Modeling - 39th International Conference. ER 2020, pp. 525–538 (2020). https://doi.org/10.1007/978-3-030-62522-1_39
- [13] Lin, Y., Yen, M., Yu, L.: Grid-based crime prediction using geographical features. *ISPRS International Journal of Geo-Information* **7**(8:298) (2018). <https://doi.org/10.3390/ijgi7080298>
- [14] Weatherburn, D.: What causes crime. *Crime and Justice Bulletin* (2001)
- [15] Glaeser, E.L., Sacerdote, B.: Why is there more crime in cities? *Journal of Political Economy* **107**(S6), 225–258 (1999). <https://doi.org/10.1086/250109>
- [16] Bappee, F.K., Petry, L.M., Soares, A., Matwin, S.: Analyzing the impact of foursquare and streetlight data with human demographics

- on future crime prediction. In: *Advances in Data Science and Information Engineering*. ICMI '14, pp. 435–449 (2021). https://doi.org/10.1007/978-3-030-71704-9_29
- [17] Almanie, T., Mirza, R., Lor, E.: Crime prediction based on crime types and using spatial and temporal criminal hotspots. *International Journal of Data Mining & Knowledge Management Process (IJDKP)* **5**(4) (2015). <https://doi.org/10.5121/ijdkp.2015.5401>
- [18] Alves, L.G.A., Ribeiro, H.V., Rodrigues, F.A.: Crime prediction through urban metrics and statistical learning. *Physica A: Statistical Mechanics and its Applications* **505**, 435–443 (2018). <https://doi.org/10.1016/j.physa.2018.03.084>
- [19] Saltos, G., Coceas, M.: An exploration of crime prediction using data mining on open data. *International Journal of Information Technology & Decision Making* **16**(5), 1155–1181 (2017). <https://doi.org/10.1142/S0219622017500250>
- [20] Sun, Y., Han, J., Yan, X., Yu, P.S., Wu, T.: Pathsim: Meta path-based top-k similarity search in heterogeneous information networks. *Proceedings of the VLDB Endowment* **4**(11), 992–1003 (2011). <https://doi.org/10.14778/3402707.3402736>
- [21] Hussein, R., Yang, D., Cudré-Mauroux, P.: Are meta-paths necessary? revisiting heterogeneous graph embeddings. In: *Proceedings of the 27th ACM International Conference on Information and Knowledge Management (CIKM)*, pp. 437–446 (2018). <https://doi.org/10.1145/3269206.3271777>
- [22] Chen, T., Yin, H., Ren, J., Huang, Z., Zhang, X., Wang, H.: Uniting heterogeneity, inductiveness, and efficiency for graph representation learning. *IEEE Transactions on Knowledge and Data Engineering* (2021). <https://doi.org/10.1109/TKDE.2021.3100529>
- [23] Wang, B., Lin, Y., Guo, S., Wan, H.: Gsnet: Learning spatial-temporal correlations from geographical and semantic aspects for traffic accident risk forecasting. In: *Proceedings of the AAAI Conference on Artificial Intelligence*, vol. 35, pp. 4402–4409 (2021)
- [24] Gers, F.A., Eck, D., Schmidhuber, J.: Applying lstm to time series predictable through time-window approaches. In: *Proceedings of the 12th Italian Workshop on Neural Nets*. Neural Nets WIRN Vietri-01, pp. 193–200 (2002). https://doi.org/10.1007/978-1-4471-0219-9_20
- [25] Bogomolov, A., Lepri, B., Staiano, J., Oliver, N., Pianesi, F., Pentland, A.: Once upon a crime: Towards crime prediction from demographics

- and mobile data. In: Proceedings of the 16th International Conference on Multimodal Interactions. ICMI '14, pp. 427–434 (2014). <https://doi.org/10.1145/2663204.2663254>
- [26] Dong, Y., Chawla, N.V., Swami, A.: Metapath2vec: Scalable representation learning for heterogeneous networks. In: Proceedings of the 23rd ACM SIGKDD International Conference on Knowledge Discovery and Data Mining. KDD '17, pp. 135–144 (2017). <https://doi.org/10.1145/3097983.3098036>
- [27] Shi, C., Hu, B., Zhao, W.X., Yu, P.S.: Heterogeneous information network embedding for recommendation. IEEE Trans. on Knowl. and Data Eng. **31**(2), 357–370 (2019). <https://doi.org/10.1109/TKDE.2018.2833443>
- [28] Fu, X., Zhang, J., Meng, Z., King, I.: Magnn: Metapath aggregated graph neural network for heterogeneous graph embedding. In: Proceedings of The Web Conference 2020. WWW '20, pp. 2331–2341 (2020). <https://doi.org/10.1145/3366423.3380297>
- [29] Li, Y., Jin, Y., Song, G., Zhu, Z., Shi, C., Wang, Y.: Graphmse: Efficient meta-path selection in semantically aligned feature space for graph neural networks. In: Proceedings of the AAAI Conference on Artificial Intelligence 2021. AAAI '21, pp. 4206–4214 (2021)
- [30] Chen, H., Yin, H., Chen, T., Nguyen, Q.V.H., Peng, W.-C., Li, X.: Exploiting centrality information with graph convolutions for network representation learning. In: 2019 IEEE 35th International Conference on Data Engineering (ICDE), pp. 590–601 (2019). <https://doi.org/10.1109/ICDE.2019.00059>
- [31] Kingma, D.P., Ba, J.: Adam: A method for stochastic optimization. In: The 3rd International Conference for Learning Representations. ICLR '15 (2015)
- [32] MuonNeutrino: Demographic, economic, and location data for census tracts in nyc. Kaggle (2017)
- [33] Department of Information Technology and Telecommunications (DOITT): Points of interest. NYC Open Data (2016)
- [34] Police Department (NYPD): Nypd complaint data historic. NYC Open Data (2016)
- [35] Green, B., Horel, T., Papachristos, A.V.: Modeling contagion through social networks to explain and predict gunshot violence in chicago, 2006 to 2014. JAMA Internal Medicine **177**(3), 326–333 (2017). <https://doi.org/10.1001/jamainternmed.2016.8245>

- [36] Huang, C., Wu, X., Zhang, X., Zhang, C., Zhao, J., Yin, D., Chawla, N.V.: Online purchase prediction via multi-scale modeling of behavior dynamics. In: Proceedings of the 25th ACM SIGKDD International Conference on Knowledge Discovery & Data Mining. KDD '19, pp. 2613–2622 (2019). <https://doi.org/10.1145/3292500.3330790>
- [37] Munnelly, G., Lawless, S.: Investigating entity linking in early english legal documents. In: Proceedings of the 18th ACM/IEEE on Joint Conference on Digital Libraries. JCDL '18, pp. 59–68 (2018). <https://doi.org/10.1145/3197026.3197055>
- [38] Jin, G., Wang, Q., Zhu, C., Feng, Y., Huang, J., Zhou, J.: Addressing crime situation forecasting task with temporal graph convolutional neural network approach. In: 2020 12th International Conference on Measuring Technology and Mechatronics Automation (ICMTMA). KDD '19, pp. 474–478 (2020). <https://doi.org/10.1109/ICMTMA50254.2020.00108>
- [39] Han, X., Hu, X., Wu, H., Shen, B., Wu, J.: Risk prediction of theft crimes in urban communities: An integrated model of lstm and st-gen. IEEE Access **8**, 217222–217230 (2020). <https://doi.org/10.1109/ACCESS.2020.3041924>
- [40] Liang, W., Wang, Y., Tao, H., Cao, J.: Towards hour-level crime prediction: A neural attentive framework with spatial–temporal–categorical fusion. Neurocomputing (2021). <https://doi.org/10.1016/j.neucom.2021.11.052>
- [41] Kipf, T.N., Welling, M.: Semi-supervised classification with graph convolutional networks. In: The 5th International Conference on Learning Representations. ICLR 2017 (2017)
- [42] Zhao, L., Song, Y., Zhang, C., Liu, Y., Wang, P., Lin, T., Deng, M., Li, H.: T-gcn: A temporal graph convolutional network for traffic prediction. IEEE Transactions on Intelligent Transportation Systems **21**(9), 3848–3858 (2020). <https://doi.org/10.1109/TITS.2019.2935152>
- [43] Deng, S., Rangwala, H., Ning, Y.: Learning dynamic context graphs for predicting social events. In: Proceedings of the 25th ACM SIGKDD International Conference on Knowledge Discovery & Data Mining. KDD '19, pp. 1007–1016 (2019). <https://doi.org/10.1145/3292500.3330919>
- [44] Yu, B., Yin, H., Zhu, Z.: Spatio-temporal graph convolutional networks: A deep learning framework for traffic forecasting. In: Proceedings of the Twenty-Seventh International Joint Conference on Artificial Intelligence. IJCAI-18, pp. 3634–3640 (2018). <https://doi.org/10.5555/3304222.3304273>

- [45] Wang, C., Lin, Z., Yang, X., Sun, J., Yue, M., Shahabi, C.: Hagen: Homophily-aware graph convolutional recurrent network for crime forecasting. In: Proceedings of the AAAI Conference on Artificial Intelligence, pp. 4193–4200 (2022)
- [46] Song, G., Bernasco, W., Liu, L., Xiao, L., Zhou, S., Liao, W.: Crime feeds on legal activities: Daily mobility flows help to explain thieves’ target location choices. *Journal of Quantitative Criminology* **35**(26), 831–854 (2019). <https://doi.org/10.1007/s10940-019-09406-z>
- [47] Rumi, S.K., Deng, K., Salim, F.D.: Theft prediction with individual risk factor of visitors. In: Proceedings of the 26th ACM SIGSPATIAL International Conference on Advances in Geographic Information Systems. SIGSPATIAL ’18, pp. 552–555 (2018). <https://doi.org/10.1145/3274895.3274994>
- [48] Rumi, S.K., Salim, F.D.: Modelling regional crime risk using directed graph of check-ins. In: Proceedings of the 29th ACM International Conference on Information & Knowledge Management. CIKM ’20, pp. 2201–2204 (2020). <https://doi.org/10.1145/3340531.3412065>
- [49] Kadar, C., Pletikosa, I.: Mining large-scale human mobility data for long-term crime prediction. *EPJ Data Science* **7**(26) (2018). <https://doi.org/10.1140/epjds/s13688-018-0150-z>
- [50] Rosés, R., Kadar, C., Malleson, N.: A data-driven agent-based simulation to predict crime patterns in an urban environment. *Computers, Environment and Urban Systems* **89**(101660) (2021). <https://doi.org/10.1016/j.compenvurbsys.2021.101660>
- [51] Wang, Z., Jiang, R., Cai, Z., Fan, Z., Liu, X., Kim, K.-S., Song, X., Shibasaki, R.: Spatio-temporal-categorical graph neural networks for fine-grained multi-incident co-prediction. In: Proceedings of the 30th ACM International Conference on Information & Knowledge Management. CIKM ’21, pp. 2060–2069 (2021). <https://doi.org/10.1145/3459637.3482482>
- [52] Park, S., Serrà, J., Martinez, E.F., Oliver, N.: Mobinsight: A framework using semantic neighborhood features for localized interpretations of urban mobility. *ACM Transactions on Interactive Intelligent Systems* **8**(3) (2018). <https://doi.org/10.1145/3158433>
- [53] Fengli Xu, Z.L., Xia, T., Guo, D., Li, Y.: Sume: Semantic-enhanced urban mobility network embedding for user demographic inference. *Proceedings of the ACM on Interactive, Mobile, Wearable and Ubiquitous Technologies* **4**(3), 1–25 (2020). <https://doi.org/10.1145/3411807>

- [54] Yang, D., Qu, B., Yang, J., Cudré-Mauroux, P.: Lbsn2vec++: Heterogeneous hypergraph embedding for location-based social networks. *IEEE Transactions on Knowledge and Data Engineering* **34**, 1843–1855 (2020). <https://doi.org/10.1109/TKDE.2020.2997869>
- [55] Huang, Y., Bi, H., Li, Z., Mao, T., Wang, Z.: Stgat: Modeling spatial-temporal interactions for human trajectory prediction. In: *Proceedings of the IEEE/CVF International Conference on Computer Vision. ICCV '19*, pp. 6272–6281 (2019). <https://doi.org/10.1109/ICCV.2019.00637>
- [56] Wang, S., Miao, H., Chen, H., Huang, Z.: Multi-task adversarial spatial-temporal networks for crowd flow prediction. In: *Proceedings of the 29th ACM International Conference on Information & Knowledge Management. CIKM '20*, pp. 1555–1564 (2020). <https://doi.org/10.1145/3340531.3412054>
- [57] Chen, T., Yin, H., Chen, H., Wu, L., Wang, H., Zhou, X., Li, X.: Tada: trend alignment with dual-attention multi-task recurrent neural networks for sales prediction. In: *2018 IEEE International Conference on Data Mining (ICDM)*, pp. 49–58 (2018). IEEE
- [58] Chen, T., Yin, H., Nguyen, Q.V.H., Peng, W.-C., Li, X., Zhou, X.: Sequence-aware factorization machines for temporal predictive analytics. In: *2020 IEEE 36th International Conference on Data Engineering (ICDE)*, pp. 1405–1416 (2020). IEEE
- [59] Tam, N.T., Weidlich, M., Zheng, B., Yin, H., Hung, N.Q.V., Stantic, B.: From anomaly detection to rumour detection using data streams of social platforms. *Proceedings of the VLDB Endowment* **12**(9), 1016–1029 (2019)
- [60] Trung, H.T., Van Vinh, T., Tam, N.T., Yin, H., Weidlich, M., Hung, N.Q.V.: Adaptive network alignment with unsupervised and multi-order convolutional networks. In: *2020 IEEE 36th International Conference on Data Engineering (ICDE)*, pp. 85–96 (2020). IEEE
- [61] Yao, H., Liu, Y., Wei, Y., Tang, X., Li, Z.: Learning from multiple cities: A meta-learning approach for spatial-temporal prediction. In: *The World Wide Web Conference. WWW '19*, pp. 2181–2191 (2019). <https://doi.org/10.1145/3308558.3313577>
- [62] Wang, H., Kifer, D., Graif, C., Li, Z.: Crime rate inference with big data. In: *Proceedings of the 22nd ACM SIGKDD International Conference on Knowledge Discovery and Data Mining*, pp. 635–644 (2016). <https://doi.org/10.1145/2939672.2939736>

- [63] Wang, T., Rudin, C., Wagner, D., Sevieri, R.: Learning to detect patterns of crime. In: Joint European Conference on Machine Learning and Knowledge Discovery in Databases (ECML), pp. 515–530 (2013). https://doi.org/10.1007/978-3-642-40994-3_33
- [64] Yang, D., Heaney, T., Tonon, A., Wang, L., Cudré-Mauroux, P.: Crime-telescope: crime hotspot prediction based on urban and social media data fusion. *World Wide Web* **21**(5), 1323–1347 (2018). <https://doi.org/10.1007/s11280-017-0515-4>
- [65] Zhao, X., Fan, W., Liu, H., Tang, J.: Multi-type urban crime prediction. In: Proceedings of the AAAI Conference on Artificial Intelligence (2022)